2016 IEEE International Conference on Advanced Intelligent Mechatronics (AIM)
Banff, Alberta, Canada, July 12–15, 2016

Partial Estimation of Needle Tip Orientation in Generalized Coordinates in Ultrasound Image-guided Needle Insertion

Bita Fallahi[1], Carlos Rossa [1], Ronald Sloboda [2], Nawaid Usmani [2], and Mahdi Tavakoli [1]

Abstract— **In many subcutaneous needle insertion procedures, measuring needle deflection is necessary in order to accurately guide the needle towards inner body targets. Typically, needle deflection measurement are obtained from 2D ultrasound images, which can only provide the needle tip position, however, having knowledge about the needle tip heading (orientation) is very valuable in predicting the needle's future path for planning and needle steering reasons. Due to the small diameter of the needles and the low resolution of ultrasound imaging, the direct measurement of the needle tip orientation is not a trivial task. This paper represents a model-based non linear observer for partial estimating the needle tip orientation during needle insertion procedures using image-based position measurements. The proposed method employs a 3D kinematic unicycle model expressed in generalized coordinates. Applying nonlinear transformations on system states, the linearized transformed system equations are utilized in the observer design procedure. However, due to the singularities imposed by these transformations, certain assumptions are made for the convergence proof of the observer. The proposed observer is tested in simulations and experiments. In experiments, the observer is fed by the needle tip position measurements, which are obtained from real-time ultrasound images.**

I. Introduction

Steerable needles have been widely used in procedures such as brachytherapy, biopsy and neurosurgery. For the aim of treatment, diagnosis or sample removal, long flexible needles are inserted into the human body.

Accurate control of the needle tip trajectory towards a target is key to the success of these procedures, however, due to the flexibility of the needles, asymmetry at the needle tip and tissue deformations, the process of steering the needle on a desired path turns out to be a challenging problem. Using needle/tissue interaction models and feedback measurements, robots can be employed to improve the accuracy of such procedures. Controlling such systems by closed-loop feedback schemes requires information such as needle shape, needle/tissue interaction forces and needle tip position, velocity, and orientation. Using different measurements, there have been various planning and control methods proposed in the literature. In some image-base methods [1] [2], the position of the needle is used as the feedback signal for motion planning in a 3D environment with obstacles. [3] has integrated online curvature estimation in 3D path planners [4]. Other papers have considered different position measurement methods such as electromagnetic tracking [5] [6] and fiber Bragg grating sensors for measuring the strain and reconstructing the needle shape [7]. In [8], needle deflection is estimated using the needle's model and forces measured at the needle base during insertion. However, inserting measurement equipment inside the human body demands equipment miniaturization and suffers from sterilization concerns. In general, it is more practical to use measurement modalities that are located outside the body (non-invasive) such as force measurements at the needle base and imaging methods such as ultrasound and CT. Image processing can provide us with information about needle shape and needle tip position in 3D space. Among different imaging modalities, ultrasound probes that contain array-type transducer are very common. Their 2D images only provide the Cartesian position of the needle tip and the needle tip orientation is not visible in such 2D ultrasound images.

Since knowledge about both needle tip position and orientation is key to planning and control, state observers, which are based on both mathematical models and sensor measurements, can be employed to estimate the non-measurable variables. [9] has used a high-gain observer to estimate the needle velocities based on noisy position data obtained from encoder measurements. [10] has designed a linear observer-based feedback control system, and used the 3D kinematic unicycle model [11] in generalized coordinates for observer design. [12] combines the same observer with other controllers. In this paper, we propose a nonlinear observer that uses Cartesian position measurement data to estimate the orientation of the needle tip as the needle is inserted into tissue. With certain assumptions and constraints on system states and inputs, the zero convergence of the proposed observer error is shown using Lyapunov-based methods. Its performance is evaluated by both simulations and experiments. Using the proposed observer the average absolute estimation error is obtained as 0.02 rad.

The paper is organized as follows. Section II presents a review of the unicycle equations used to model the needle deflection in tissue in generalized coordinates. Section III presents the observer structure, the assumptions and the convergence proof of the observer are represented in Section IV. In Section V, the proposed observer is validated using simulations and the experimental results are presented in

This work was supported by the Natural Sciences and Engineering Research Council (NSERC) of Canada under grant CHRP 446520, the Canadian Institutes of Health Research (CIHR) under grant CPG 127768, and by the Alberta Innovates - Health Solutions (AIHS) under grant CRIO 201201232.

[1]B. Fallahi, C. Rossa, PhD, and M. Tavakoli (Corresponding Author), PhD, are with the Department of Electrical and Computer Engineering, University of Alberta, Edmonton, Canada T6G 2V4. E-mail: {fallahi, rossa, madhi.tavakoli}@ualberta.ca

[2]R. Sloboda and N. Usmani are with the Cross Cancer Institute and the Department of Oncology, University of Alberta, Edmonton, Edmonton, Canada T6G 1Z2. E-mail: {ron.sloboda, nawaid.usmani}@albertahealthservices.ca.

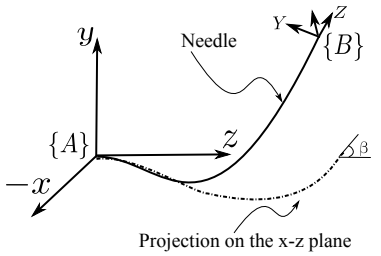

Fig. 1. The needle shown in 3D space. The frame $\{A\}$ is the fixed frame and the moving frame $\{B\}$ is attached to the needle tip.

Section VI.

II. Background

As a beveled-tip needle is inserted into tissue, due to the bevel at its tip, the needle bends and moves on a curved path in 3D space. The orientation of the bevel is a key element in determining the traversed trajectory. Axial rotation of the needle at its base can be considered as an input to steer the needle to the desired position. Assuming the needle rotation velocity as the input, the kinematics of a bevel tip needle inserted into tissue can be expressed using unicycle equation in 3D space [5] which can be represented using $Z-Y-X$ fixed angles as generalized coordinates [10] as:

$$\dot{x} = v\sin\beta, \tag{1a}$$
$$\dot{y} = -v\cos\beta\sin\alpha, \tag{1b}$$
$$\dot{z} = v\cos\alpha\cos\beta, \tag{1c}$$
$$\dot{\alpha} = kv\cos\gamma\sec\beta, \tag{1d}$$
$$\dot{\beta} = kv\sin\gamma, \tag{1e}$$
$$\dot{\gamma} = -kv\cos\gamma\tan\beta + u \tag{1f}$$

The generalized coordinates $q = \begin{bmatrix} x & y & z & \alpha & \beta & \gamma \end{bmatrix}$ is well defined on

$$\mathcal{U} = \{q \in \mathbb{R}^6 : \alpha, \gamma \in \mathbb{R}, \beta \in (-\pi/2, \pi/2)\} \tag{2}$$

In (1) $(\dot{\times})$ denotes the time derivative and $\begin{bmatrix} x & y & z \end{bmatrix}^T$ represents the position of the moving frame $\{B\}$ attached to the needle tip with respect to the fixed frame $\{A\}$ as shown in Fig. 1. α, β and γ represent the yaw, pitch and roll angles (orientation) of the needle, respectively. In these equations k, v and u denote the needle path curvature, insertion velocity and axial rotation velocity, respectively. It should be noted that, using ultrasound images, only x, y and z can be measured and the other three angles, which determine the needle tip orientation, are not measurable. In the next section a nonlinear observer is proposed by which the roll and pitch angles can be estimated.

III. Observer

A. Observer equations

Consider the following transformation:

$$s = \begin{bmatrix} x \\ \sin\beta \\ -\cos\beta\sin\gamma \end{bmatrix} \tag{3}$$

from which the pitch and roll angles can be found as

$$\beta = \arcsin(s_2) \tag{4a}$$
$$\gamma = atan2(-s_3/\cos\beta, \cos\gamma) \tag{4b}$$

where $atan2(a,b)$ is the function that calculates $\arctan(\frac{b}{a})$ taking the sign of both arguments into account. It is easy to see that $\cos\gamma$ can be found as

$$\cos\gamma = \zeta\frac{\sqrt{1-(s_2^2+s_3^2)}}{\cos\beta} \tag{5}$$

where $\zeta = sign(\cos\gamma)$ depends on the bevel orientation. Moreover, from (2) we have $\cos\beta > 0$. Using (3), the transformed system equations can be written as

$$\dot{s} = \begin{bmatrix} vsin\beta \\ -kv\cos\beta\sin\gamma \\ kv\sin\beta - u\cos\beta\cos\gamma \end{bmatrix} = \begin{bmatrix} vs_2 \\ -kvs_3 \\ kvs_2 - \zeta u\sqrt{1-(s_2^2+s_3^2)} \end{bmatrix}$$
$$y = \begin{bmatrix} 1 & 0 & 0 \end{bmatrix} s = x \tag{6}$$

in which the deflection of needle tip in the x direction has been considered as the output and the needle rotation velocity u acts as the input. The system equations can be re-written in the form

$$\dot{s} = As + \phi(u,s) \tag{7}$$

with

$$A = \begin{bmatrix} 0 & v & 0 \\ 0 & 0 & -vk \\ 0 & 0 & 0 \end{bmatrix} \tag{8a}$$

$$\phi(u,s) = \begin{bmatrix} 0 \\ 0 \\ kvs_2 - \zeta u\sqrt{1-(s_2^2+s_3^2)} \end{bmatrix} \tag{8b}$$

Now consider the following observer [13]

$$\dot{\hat{s}} = A\hat{s} + \phi(u,\hat{s}) + \Delta_\theta L(\hat{y} - y) \tag{9}$$

where $L = \begin{bmatrix} L_1 & L_2 & L_3 \end{bmatrix}^T$ is the observer gain, which should be selected such that $A + LC$ is Hurwitz, and

$$\Delta_\theta = diag\{\theta, \theta^2, \theta^3\} \tag{10}$$

with $\theta > 1$.

IV. Convergence of the Observer

A. Convergence

In this section, it is shown that under certain assumptions and by proper choice of the observer gain, the observation error will tend to zero. To show the convergence of the proposed observer, define the observation error as $e = \Delta_\theta(\hat{s} - s)$. Using the system equation (7) and observer equation (9), we have

$$\dot{e} = \theta(A + LC)e + \Delta_\theta^{-1}\delta_\phi(u,s) \tag{11}$$

with $\delta_{\phi 1}(u,s) = \delta_{\phi 2}(u,s) = 0$ and

$$\delta_{\phi 3}(u,s) = kv(\hat{s_2} - s_2) + \zeta u(\sqrt{1-(\hat{s}_2^2+\hat{s}_3^2)} - \sqrt{1-(s_2^2+s_3^2)}) \quad (12)$$

If the nonlinear term $\delta_\phi(u,s)$ is a Lipschitz function, i.e. $\exists c > 0$ such that $\|\phi(u,s) - \phi(u,s')\| \leq c\|s - s'\|$, where $\|.\|$ denotes the euclidean norm of $\mathbb{R}^n$, for $\theta > 1$, equation (9) forms an exponential observer [13]. However, since the function $\sqrt{1-(s_2^2+s_3^2)}$ does not satisfy the Lipschitz continuity condition as $(s_2^2+s_3^2) \to 1$, using the fact that $|s_i| \leq 1$ $(i = 2, 3)$, assume

$$\sqrt{1-(s_2^2+s_3^2)} \geq \epsilon \quad (13)$$

due to which (12) can be upper bounded as

$$|\delta\phi(3)| \leq \frac{\bar{u}}{2\epsilon}((\hat{s}_2^2 - s_2^2) + (\hat{s}_3^2 - s_3^2)) + kv|\hat{s_2} - s_2| \quad (14)$$

where $\bar{u} > 0$ is the upper bound for the input signal u. (14) can be simplified to

$$|\delta\phi| \leq (kv + \frac{\bar{u}}{\epsilon})\|e\| \quad (15)$$

Now consider the Lyapunov function

$$V(e) = \frac{1}{2}e^T P e \quad (16)$$

with P being a positive definite matrix. Since L is chosen such that $A + LC$ is Hurwitz, then P can be found as the response of the algebraic Lyapunov equation $(A+LC)^T P + P(A+LC) = -I$. We have

$$\dot{V} = -\theta\|e\|^2 + 2e^T P\delta\phi(s,u) \quad (17)$$

From (15) the above equality can be written as

$$\dot{V} \leq (-\theta + 2\|P\|(\frac{\bar{u}}{\epsilon} + kv))\|e\|^2 \quad (18)$$

Choosing $\theta > 2\|P\|(\frac{\bar{u}}{\epsilon} + kv)$ leads to $\dot{V} < 0$.

B. Assumptions and Constraints

In the previous section, the convergence of the proposed observer was shown for the region obtained from (13). However if $\sqrt{1-(s_2^2+s_3^2)} \to 0$, which is equivalent to $|\sin\beta| \to 1$ or $|\sin\gamma| \to 1$, there is no guarantee for convergence of the estimation error at these points as the Lipschitz continuity condition is not satisfied. However if the observer is combined with path planning methods and/or controllers, it is possible to use the proposed observer. The kinematic equations (1) are well defined on $\mathcal{U}$ in (2). If path planners are employed to steer the needle on a desired path, $\beta = \pm\frac{\pi}{2}$ can be avoided in planning level. On the other hand, since γ is directly related to the input u, it may have any value. Moreover, to have $\cos\gamma > 0$ or $\cos\gamma < 0$, which affects the needle path in the y-direction, the angle γ should pass the critical point $\cos\gamma = 0$, meaning that it is not possible to limit the angle γ to $[-\pi/2, \pi/2]$. Nevertheless, in practice, if the input u is designed such that $\gamma = n\pi/2$ is only a transient via point and the goal is to keep γ at angles other that $n\pi/2$, then the proposed observer can be used to estimate the angles β and γ and the convergence of the observation error to zero is guaranteed.

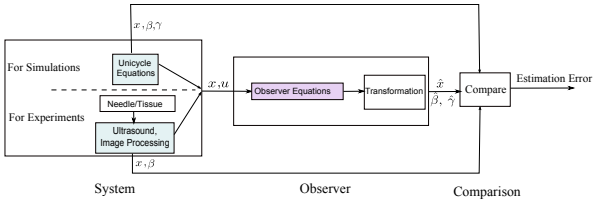

Fig. 2. Block diagram of the observation system for (a): Simulation, (b): experiments

C. Implementation Considerations

According to (9), in order to avoid any numerical problems in implementing the observer equations, the term $1-(\hat{s}_2^2+\hat{s}_3^2)$ should always be positive, so in any case that this condition is not satisfied, this term is substituted by zero. Moreover, from (4) for finding γ, ζ should be known which changes as the angle γ passes the points $n\pi/2$ which is equivalent to $\sqrt{1-(\hat{s}_2^2+\hat{s}_3^2)} = 0$. Since it is assumed that the critical point $\gamma = n\pi/2$ is a transient via point, by having the initial value of γ, the condition $\sqrt{1-(\hat{s}_2^2+\hat{s}_3^2)} < \epsilon$ can be used to determine ζ.

V. Simulations

In this section, simulation results are presented to evaluate the performance of the proposed observer. As shown in Fig. 2 The system and observer are simulated using the kinematic unicycle equations (1) and observer equations (9), respectively. The simulations are performed for the insertion velocity $v = 2$ mm/sec and the needle path curvature $k = 0.0019\ mm^{-1}$ for system and $k = 0.002\ mm^{-1}$ for the observer to simulate 5% modeling error for this parameter. The inputs to the observer are the input signal u (needle rotation velocity) and the needle tip position in the x direction and the outputs are transformed system states $\hat{s}$, from which the angles β and γ can be calculated using (4). In simulations, the value of γ is controlled to have different values other than $n\pi/2$. The observer gain is selected to be $L = [-100\ -1.05\ 1.37]$ to make the matrix $A+LC$ Hurwitz $\theta = 6\pi \times 10^4$. The initial values for x and β is considered to be zero and for γ is $3°$. The results are shown in Fig. 4. The results show a maximum estimation error of 10^{-14} mm and 10^{-7} rad for x and β and a maximum estimation error of 0.05 rad for γ. The results show the convergence of the proposed observer for the considered region.

VI. Experiments

This section shows the results from implementing the proposed observer in real-time for estimating the angles β and γ as the needle is inserted into phantom tissue. The experimental setup used for conducting the experiments is shown in Fig. 3 which is a 2-DOF prismatic-revolute robotic system to insert and axially rotate the needle. The base of the needle (attached to a DC motor to axially rotate the needle) is instrumented with a force sensor not used in these experiments. The position of this needle rotation motor is controlled using a PID controller. The needle base's angle is measured by an encoders whose time derivative is considered

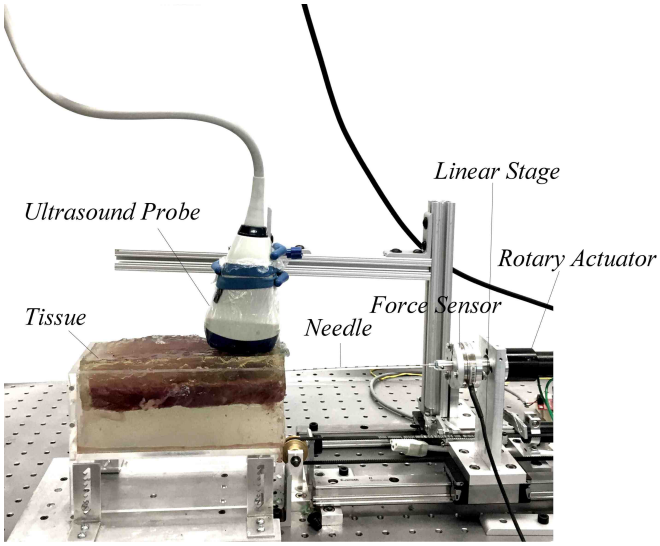

Fig. 3. Experimental setup used to perform needle insertion experiments. The setup provides translational and rotational motions of needle. An ultrasound machine (SonixTouch, Ultrasonix, BC, Canada) is used to track the needle tip position.

as the input signal u in (1). This motor is assembled on a translational stage actuated by another DC motor. In these experiments, the needle is a standard 18-gauge brachytherapy needle (Eckert & Ziegler BEBIG Inc., Oxford, CT, USA) made of stainless steel with a bevel angle of approximately 20°. The phantom tissue used in these experiments is a 15% gelatin mixture made by mixing gelatin powder (Sigma-Aldrich Co., ON, Canada) and $70^\circ C$ water. As the needle is inserted, an ultrasound probe tracks the needle tip and acquires 2D transverse images of the needle tip. Using these transverse images, the needle tip position is estimated using the random sample consensus (RANSAC) technique [14]. In the experiments, the control algorithm proposed in [15] is employed in which the main goal is compensating for the needle deflection in y direction by 180° axial rotations at appropriate depths. This method only requires the needle deflection in the y direction. The needle path curvature is selected as $0.002\ mm^{-1}$ which is obtained by fitting a circle to the deflection data obtained by inserting the needle into tissue without any axial rotations. The insertion velocity in the experiments is 2 mm/sec and the maximum insertion depth is 100 mm. The experiments are performed 6 times. The observer gain L is identical to the values used in the simulations and $\theta = 10^6$.

The evaluation is performed by comparing the estimated variables with the real values obtained from experiments. As stated before, only the position of the needle tip can be measured from 2D ultrasound images and the angles β and γ can not be measured in real-time. However, the angle β can be considered as the angle between the Z axis of the moving frame $\{B\}$ with respect to the z axis of the fixed frame $\{A\}$ in $x-z$ plane, which can be found by off-line curve fitting on position data. However, there is no way for measuring the angle γ from 2D ultrasound images. The results are shown in Fig. 5. This figure represents the estimation error for position in the x direction and the the angle β for 6 trials. In this figure, to compensate for noisy position measurements, polynomials are fitted to the position data and the real value β is calculated at each insertion depth. The observer response is also smoothed by fitting polynomials to the estimated value $\hat{\beta}$, as shown in Fig. 5 . The results are summarized in Table I, which shows the performance of the observer in estimating the position in the x direction and the angle β representing average errors of 2×10^{-14} mm and 0.02 rad, respectively. Due to impossibility of measuring the real value of the angle γ using the current equipment, this value is not shown in the figures.

TABLE I

SUMMARY OF THE EXPERIMENTAL RESULTS

	Average Absolute Estimation Error	MRSE	Standard Deviationσ
e_x[mm]	2e-14	5e-13	5e-13
e_β[rad]	0.02	0.04	0.037

VII. CONCLUSION

In this paper, we have presented an observer for partially estimating the needle tip orientation during insertion. In this method, nonlinear transformations are applied on a 3D unicycle model of the needle, based on the observer equations are formed. The inputs to the observer are the input signal u (needle rotation velocity) and the position measurements in x direction which is obtained from 2D ultrasound images. Due to the singularities imposed by the nonlinear transformations, the convergence of the observer is shown under some assumptions and constraints. The evaluation of the observer is performed using simulations and experiments. The simulations are performed using the 3D unicycle equations as the real system while the value of the needle path curvature parameter used in system equations is different from the value used in the observer equations. The experiments are performed by inserting the needle into phantom tissue using an experimental setup. The position x measurements are obtained from 2D transverse ultrasound images. From this, the real value of the needle tip pitch angle β is calculated using curve fitting techniques. Then, the estimated variables $\hat{x}$ and $\hat{\beta}$ are compared to these real values.

The proposed observer in this paper is able to estimate the needle tip orientation in terms of β and γ and the yaw angle α can not be estimated using this structure. Moreover, in this formulation, the critical points limit the observer to some extent. Further developments and different observer structures are required to overcome these issues, which remains as our future goals.

REFERENCES

[1] J. Xu, V. Duindam, R. Alterovitz, and K. Goldberg, "Motion planning for steerable needles in 3d environments with obstacles using rapidly-exploring random trees and backchaining," in *IEEE International Conference on Automation Science and Engineering, CASE 2008.* IEEE, 2008, pp. 41–46.

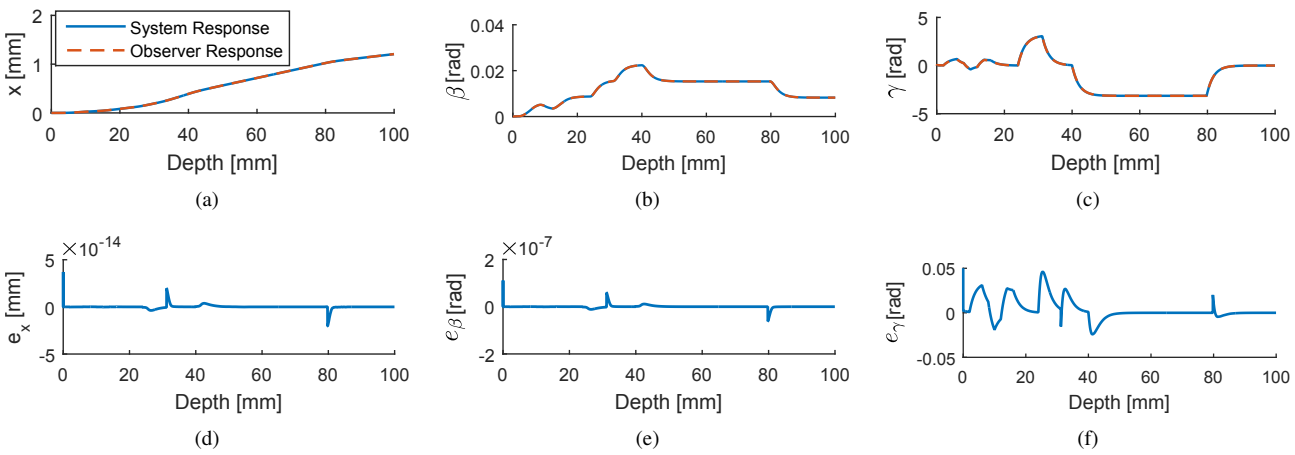

Fig. 4. Simulation results using unicycle equations and the proposed observer (a),(b),(c): the system and observer response for x, β and γ. (d),(e),(f): estimation error

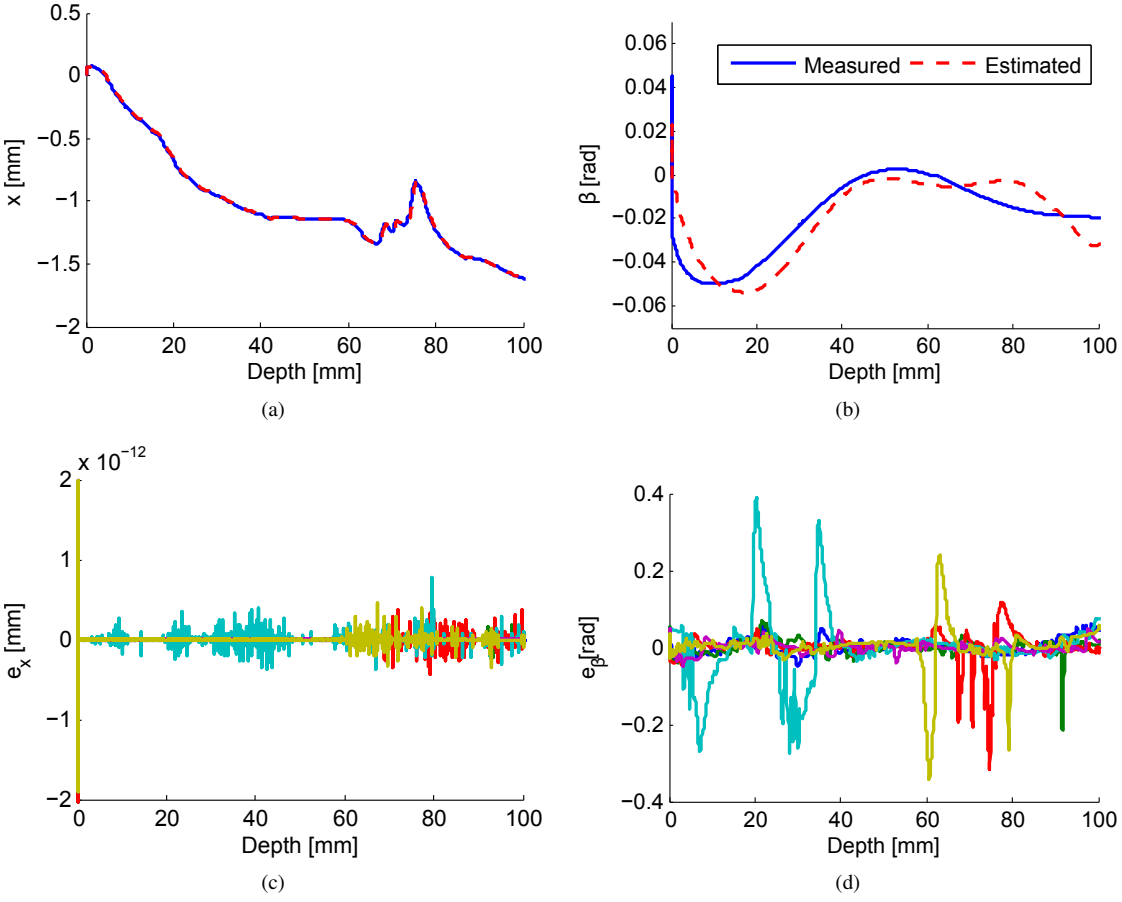

Fig. 5. Experimental results for needle insertion and observer state estimation for gelatin tissue and insertion velocity of 2 mm/sec and insertion depth of 100 mm . (a) demonstrates the estimated position in x direction as well as the real values for one of the trials. (b) demonstrate the polynomial fitted values of estimated and real value of pitch angle for one of the trials. (c),(d), show the estimation error for the trials.

[2] V. Duindam, R. Alterovitz, S. Sastry, and K. Goldberg, "Screw-based motion planning for bevel-tip flexible needles in 3d environments with obstacles," in *IEEE International Conference on Robotics and Automation, ICRA 2008*. IEEE, 2008, pp. 2483–2488.

[3] P. Moreira, R. Patil, R. Alterovitz, and S. Misra, "Needle steering in biological tissue using ultrasound-base online curvature estimation," in *& International Conference on Robotics and Automation (ICRA), 2014*. IEEE, 2014.

[4] D. S. Minhas, J. A. Engh, M. M. Fenske, and C. N. Riviere, "Modeling of needle steering via duty-cycled spinning," in *29th Annual International Conference of the IEEE Engineering in Medicine and Biology Society, 2007. EMBS 2007*. IEEE, 2007, pp. 2756–2759.

[5] D. C. Rucker, J. Das, H. B. Gilbert, P. J. Swaney, M. I. Miga, N. Sarkar, and R. J. Webster, "Sliding mode control of steerable needles," 2013.

[6] N. Shahriari, E. Hekman, M. Oudkerk, and S. Misra, "Design and evaluation of a computed tomography (ct)-compatible needle insertion device using an electromagnetic tracking system and ct images," *International journal of computer assisted radiology and surgery*, pp. 1–8, 2015.

[7] M. Abayazid, M. Kemp, and S. Misra, "3d flexible needle steering in soft-tissue phantoms using fiber bragg grating sensors," in *IEEE International Conference on Robotics and Automation, ICRA 2013*. IEEE, 2013, pp. 5843–5849.

[8] N. Abolhassani, R. V. Patel, and F. Ayazi, "Minimization of needle deflection in robot-assisted percutaneous therapy," *The international journal of medical Robotics and computer assisted surgery*, vol. 3, no. 2, pp. 140–148, 2007.

[9] A. Asadian, R. V. Patel, and M. R. Kermani, "A distributed model for needle-tissue friction in percutaneous interventions," in *IEEE International Conference on Robotics and Automation (ICRA), 2011*. IEEE, 2011, pp. 1896–1901.

[10] V. Kallem and N. J. Cowan, "Image guidance of flexible tip-steerable needles," *IEEE Transactions on Robotics*, vol. 25, no. 1, pp. 191–196, 2009.

[11] R. J. Webster, J. S. Kim, N. J. Cowan, G. S. Chirikjian, and A. M. Okamura, "Nonholonomic modeling of needle steering," *The International Journal of Robotics Research*, vol. 25, no. 5-6, pp. 509–525, 2006.

[12] M. Motaharifar, H. A. Talebi, A. Afshar, and F. Abdollahi, "Adaptive observer-based controller design for a class of nonlinear systems with application to image guided control of steerable needles," in *American Control Conference (ACC), 2012*. IEEE, 2012, pp. 4849–4854.

[13] G. Besançon, *Nonlinear observers and applications*. Springer, 2007, vol. 363.

[14] M. Waine, C. Rossa, R. Sloboda, N. Usmani, and M. Tavakoli, "3d shape visualization of curved needles in tissue from 2d ultrasound images using ransac," in *IEEE International Conference on Robotics and Automation, ICRA 2015*. IEEE, 2015, pp. 4723–4728.

[15] B. Fallahi, C. Rossa, R. Sloboda, N. Usmani, and M. Tavakoli, "Sliding-based switching control for image-guided needle steering in soft tissue," *IEEE Transactions on Robotics and Automation Letters,*, 2016.